Evaluation of Possible Corrosion Enhancement Due to Telluric Currents: Case Study for Brazil Bolivia – Pipeline

Joyrles Fernandes de Moraes[1], Igo Paulino[2], Livia Alves[3], and Clezio Marcos Denardini[4]

[1]Departamento de Engenharia de Petróleo, Universidade Estadual de Campinas, Campinas, Brazil
[2]Unidade Acadêmica de Física, UFCG, Campina Grande, Brazil
[3]Divisão de Geofísica Espacial, INPE, São José dos Campos, Brazil
[4]Divisão de Aeronomia, INPE, São José dos Campos, Brazil

Correspondence: Joyrles F. Moraes (joyrles1996@gmail.com)

Abstract. Electric field induced in the "Brazil – Bolivia" pipeline was calculated using a distributed source line transmission (DSLT) theory during several space weather events. We used geomagnetic data collected by a fluxgate magnetometer located at São José dos Campos ($23.2^oS; 45.9^oW$). The total corrosion rate was calculated using the Gummow (2002) methodology and based on the assumption of 1-cm hole in pipeline coating. The calculations were performed for the ends of pipeline, where the largest "out of phase" pipe-to-soil potential (PSP) variations were obtained. The variations in PSP during the 17th March 2015 magnetic storm have led to the greatest corrosion rate of the analysed events. All the space weather events evaluated with high terminating impedance may have contributed to increase the corrosion process. The applied technique can be used to evaluate the corrosion rate due to the high telluric activity associated with the geomagnetic storms at specific locations.

1   Introduction

Telluric electric currents that flow within the Earth or on its surface are significantly enhanced during disturbances of the Earth's magnetic field (magnetic storms).These currents can propagate through conducting systems at the Earth's surface, such as, pipelines (Campbell Alaska pipeline), phone cables (Anderson et al., 1974), and electrical power systems (Lanzerotti et al., 1999), which can produce blackouts in extreme events (Guillon et al., 2016).

The Geomagnetic Induced Currents (GICs) propagation throughout pipelines can changes the pipe-to-soil potential (PSP) which changes the electrochemical environment on the pipeline surface, which can take to a corrosion process. In pipelines cathodically protected, the PSP is maintained at negative potential of at least -850 mV. Fluctuations in PSP caused by GICs can lead the potential beyond -850 mV, resulting in corrosion (Seager, 1991). According to Place and Sneath (2001), PSP fluctuations also interfere in pipeline surveys.

Previous works on GICs were done in high latitudes, which revealed specific interactions of geomagnetic field with solar wind disturbances (Campbell, 1980; A. Fernberg et al., 2007). Effects of GICs in pipelines have been observed and published

also in Argentina (Osella et al., 1998), Australia (Marshall et al., 2010) and New Zealand (Ingham and J. Rodger, 2018), where engineers had tried to find ways to dealing with the problem.
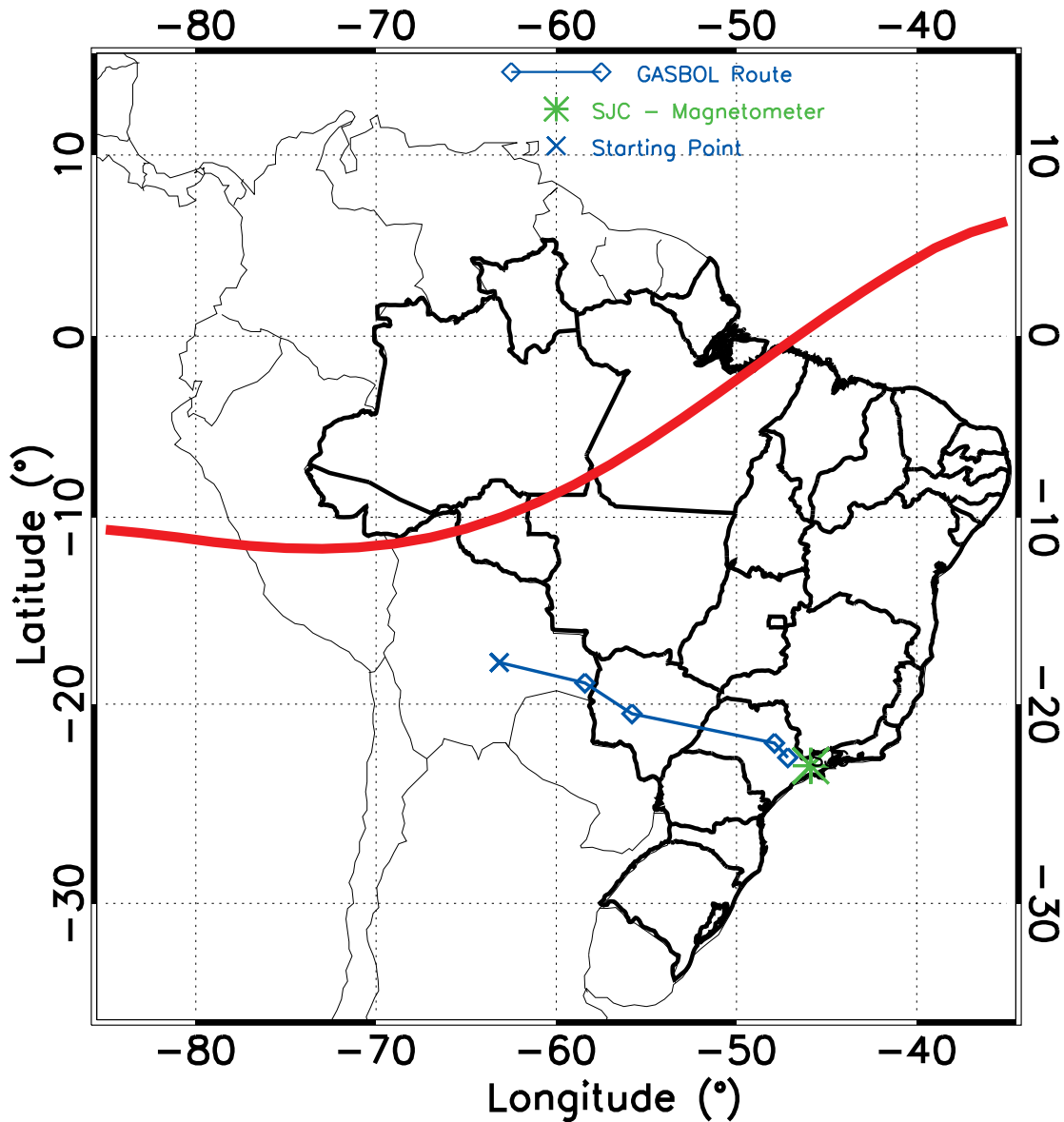
Boteler and Cookson (1986) have shown that the telluric voltage induced on pipelines can be calculated using distributed source transmission line (DSTL) equations and telluric effects in pipeline is influenced not only by space weather events, but it is also depend on the Earth's conductivity, the pipeline electromagnetic properties and geometric parameters. These calculations, when applied to modern well-coated pipelines, suggest that telluric current effects may not be as innocuous as originally thought especially for long pipelines located in high latitudes (Gummow, 2002). The DSTL theory was first described in Schelkunoff (1943) and has been used in several studies (Pulkkinen et al., 2001).

In this paper, the model for induced effects in pipelines proposed by Trichtchenko and Boteler (2002), using the DSTL theory, is used to compute the corrosion rates in Bolivia-Brazil gas pipeline (GASBOL) during specific space weather events with focus on 17th March 2015 Geomagnetic Storm. The GASBOL is the largest pipeline in Latin America, with a total extension of 3,159 km, extending from Rio Grande, Bolivia, to Canoas, Brazil. The pipeline runs through 557 km up to Brazilian border. It is the main mode of gas transportation in Brazilian territory. The GASBOL is buried about 0.5 m in the ground to ensure its integrity.

2 Instrumentation and Methodology

2.1 Magnetometer

The Earth's magnetic field and its variations are recorded at geomagnetic observatories and stations all over the globe. In the present manuscript, we have used magnetic measurements from São José dos Campos (23.2^{o}S; 45.9^{o}W) station to study the corrosion produced by GICs in the first GASBOL route (Rio Grande (17.8^{o}S; 63.1^{o}W) to Paulinia (22.8^{o}S; 47.1^{o}W) which has 1,814 km of length. The location of the GASBOL route under study and the magnetic station location are shown in Figure (the red line represents the geomagnetic equator).

Figure 1. Bolivia - Brazil Gas Pipeline Route(solid line), bends(diamonds) and São José dos Campos (23.2^oS; 45.9^oW) Magnetic Observatory (star).The red line represents the geomagnetic equator. The route length is 1814 km. The pipeline runs through 557 km up to Brazilian border. The pipeline starts in Bolivia and it is represented by "x".

We chose 8 events to study the effects of space weather in the pipe with different intensities. The events was chosen based on Disturbed Storm Time Index (DST), as it is shown in Table 1.

Table 1. DST Index of the events in 2015.

Date	17/03	23/06	07/11	09/01	27/04	07/02	03/08	27/10
$DST_{min}(nT)$	-222	-204	-89	-62	-29	-25	Quiet day	Quiet day

São José dos Campos' magnetic station is part of the Embrace MagNet and it is operated by the Brazilian Studies and Monitoring of Space Weather (Embrace/INPE). The Embrace MagNet cover most of the eastern South American longitudinal sector (Denardini et al., 2015). This network fills the gap with magnetic measurements available online in this sector and aims to provide magnetic data to be used to study changes in space weather. All the details on the magnetic network, type of magnetometers, data resolution, data quality control, and data availability have been published elsewhere (Denardini et al., 2018).

2.2   Electric Field

The electric fields produced by geomagnetic disturbances drive electric currents into the Earth. These currents are responsible for fluctuations in PSP. According to Trichtchenko and Boteler (2002), GICs have the effect of shielding the interior of the Earth from the geomagnetic disturbance. As the magnetic and electric fields are dependents on the conductivity structure of the Earth, the variation of the conductivity with depth was modeled using multiple horizontal layers with a different uniform conductivity. The Earth model layersused in this paper was obtained in São José dos Campos in previous geophysical surveys and published by Padilha et al. (1991) and are shown in Table 2.

Table 2. Multiple Horizontal Layers Model.

Layers	1	2	3	4	5	6
Thickness(m)	0.2	10	2	20	200	-
Resistivity(Ω.m)	160	12	5000	500	5000	300

The electric field on the surface can be obtained by

$$E_{surface} = zH_{surface} \tag{1}$$

where H is the magnetic field component obtained from the magnetometer and z is the surface impedance obtained by applying the recursion relation for the impedances at the multiple horizontal layers (Trichtchenko and Boteler, 2002). In our case, we are considering z as a scalar, hence, the $E_{surface}$ is orthogonal to $H_{surface}$.

2.3 DSTL Theory

The electrical response of a pipeline can be modeled by the DSTL equations. In the DSTL approach, each uniform section of the pipeline is represented by a transmission line circuit element with specific series impedance and a parallel admittance. The voltage in any section of the pipeline can be calculated applying Trichtchenko and Boteler (2002) equation, i.e.,

$$V_p = E_p/\gamma(A_p e^{-\gamma(x-x_1)} - B_p e^{-\gamma(x_2-x)})) \tag{2}$$

where E_p is the electric field induced in the pipe, x_1 and x_2 are the positions of the ends of the pipeline, and γ is the propagations constant along the pipeline, defined as $\gamma = \sqrt{ZY}$, and $Y = G + iwC$ is the parallel admittance and $Z = R + iwL$ is the series impedance per unit length with G being the conductance to ground, C the capacitance, R the resistance of pipeline steel and L the inductance.

Equation (2) is a solution of a partial differential equation, then A_p and B_p are constants dependent on the boundary conditions at the ends of the pipeline. According to Trichtchenko and Boteler (2002), the pipeline is independent of frequency, for that reason, C and L, were not necessary to apply the theory. From the same argument, we can consider the $E_p = E_{surface}$

According to Trichtchenko and Boteler (2002), 0.1 ohms means low resistance connection to ground, and 1000 ohms means no ground connection. Since the termination impedances are unknown in our case, we considered 5 terminating impedances (0.1 ohms, 1 ohm, 10 ohms, 100 ohms, and 1000 ohms). The circuit characteristics of GASBOL were obtained from the company website and material manufacturers for the pipeline industry and they are shown in Table 3 .

Table 3. GASBOL Technical Informations.

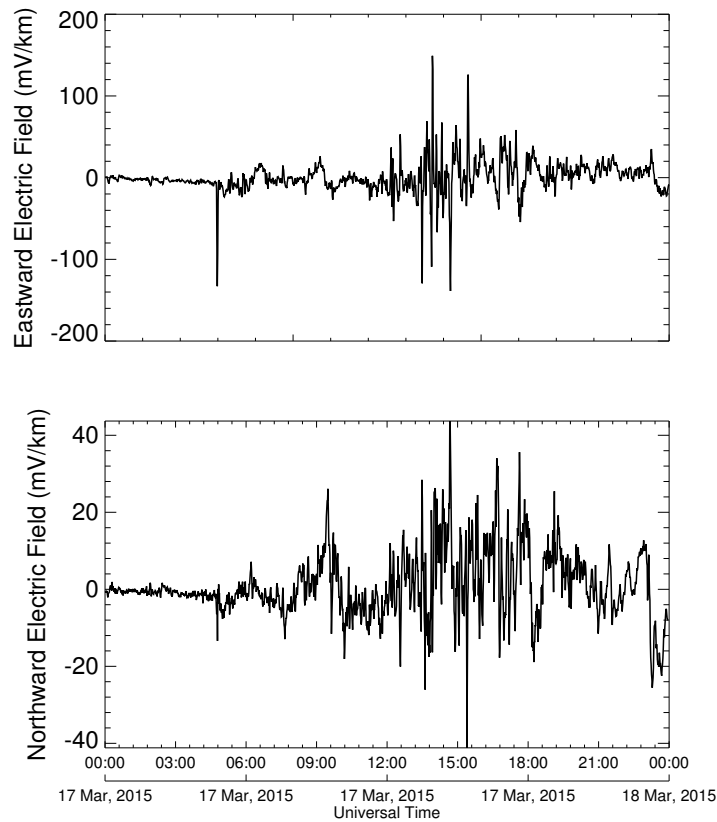| Coating thickness(in)	0.156
Coating conductivity(S/m^2)	10^{-6}
Diameter(in)	32
Steel thickness(in)	0.5
Steel resistivity(Ω.m)	2.10^{-7}

2.4 Corrosion Rate Estimation

Gummow (2002) suggested a general expression to estimate the corrosion rate (in mm/year) through a 1 cm diameter hole in pipeline coating given by:

$$CR = 31.25 V F(p) F(t) \tag{3}$$

where V is the change in PSP, $F(p)$ is the percentage of direct corrosion current due to an alternating current in a given period, and $F(t)$ is the fraction of time for which the pipe was unprotected, which is dependent of the geomagnetic activity. Gummow (2002) quoted 0.025 mm/year as the generally acceptable maximum value for corrosion rate in a pipeline. In this work, the CR was computed only for cases when the cathodic protection level was greater than -850 mV.

5

3 Results and Discussion

Figure 2 shows the electric field obtained during the 17th March 2015 magnetic storm. The electric field was obtained using Equation 1. The eastward electric field was greater than 0.15 V/km, and the northward electric field reached 0.05 V/km. These peaks were observed during the main stage of the magnetic storm. The larger values in the east component occur because the variation in a geomagnetic component leads to a change in the electrical component in perpendicular direction. For this event, the magnetic component By (north direction) presented the greatest values.

Figure 2. Eastward (top) and Northward (bottom) Electrical Field obtained by Magnetic Data on 17th March 2015 Geomagnetic Storm.

The geomagnetic field variation rate is a function of the latitude where the measurements are made and the ionospheric current system, which can affect the amplitudes of the variations. According to Trivedi et al. (2005) large amplitudes of the magnetic horizontal component can be caused by the increase of electron precipitation in the South Atlantic Magnetic Anomaly (SAMA) region , which is present in the south part of Brazil. The SAMA is a region with a low geomagnetic field intensity,
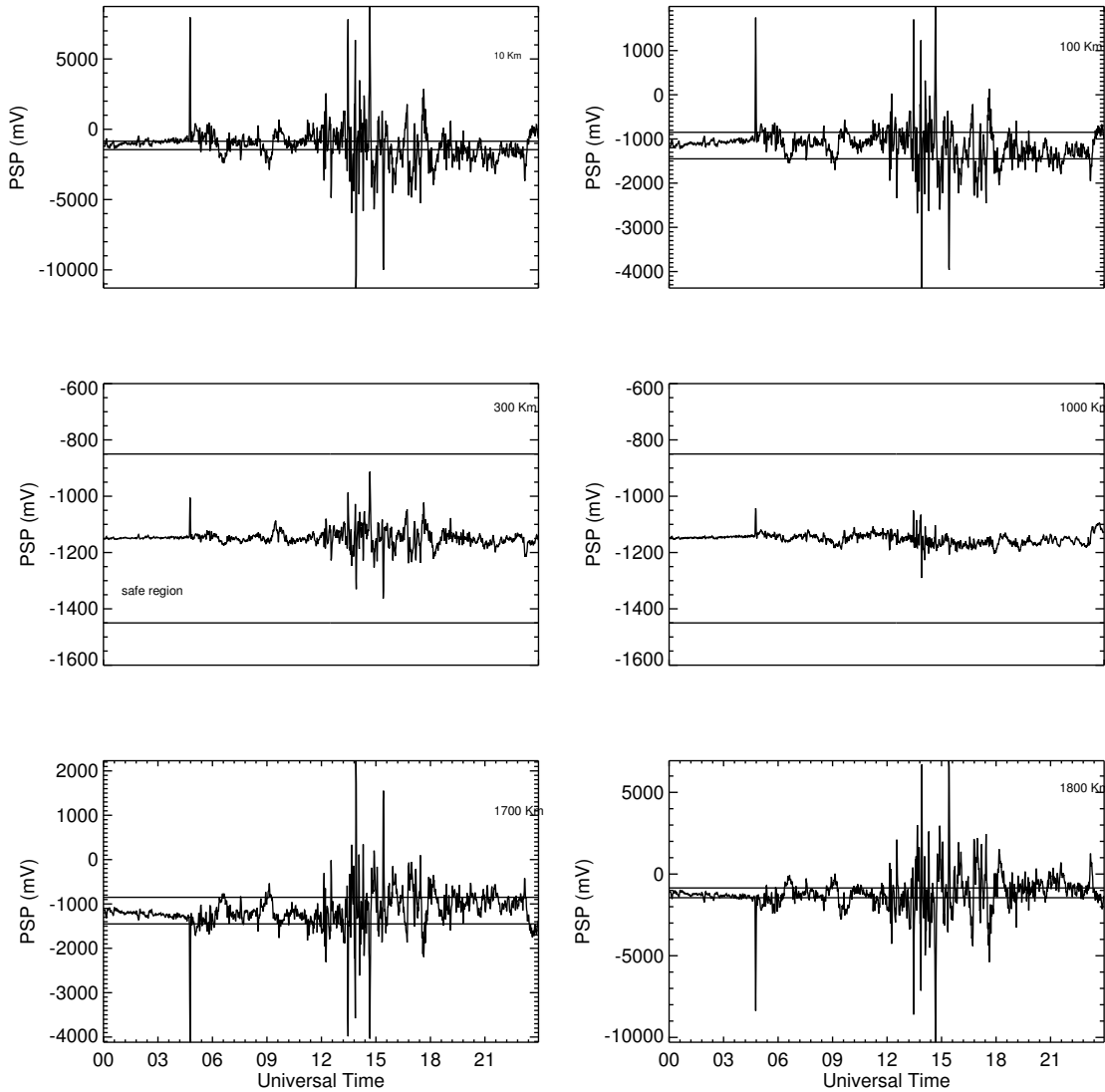
therefore it is a major point of entrance of high energy particles (Heirtzler, 2002). This region also coincides with a region in space with the intensive presence of radiation which that comes from particles that was trapped in Earth's inner Van Allen radiation belt. According to Paulikas (1975) ionospheric ionization is produced in the E layer when energetic particles come closest to the Earth's surface and interact with the dense atmosphere. This procedure increases the ionospheric conductivity which leads to the rise of the GIC intensity during disturbed periods.

Variations in the magnetic field, that cause changes in the electric field, create GICs, which are responsible for PSP fluctuations. The PSP was computed for each point in the GASBOL using Equation (2). Figure 3 shows the PSP at different sites of the pipeline with low terminating impedance (0.1 ohms). This site represents a position in the pipeline, that begins in $x = 0$ km, which is in Bolivia side, and ends in $x = 1814$ km, which represents the total extension of the first route of the pipeline. Figure 4 also contains the PSP at different sites with high terminating impedance (1000 ohms). The constants lines are the safe operating region of the pipeline (-0.85 V and -1.45 V).

Figure 3. Pipe-to-soil potential obtained by DSLT theory for different sites (values in km at the top) on the GASBOL pipeline for a terminating impedanceof 0.1 ohms on 17th March 2015 Geomagnetic Storm. Solid lines delimit the safe range of the GASBOL operation. The route has a total extension of 1814 km and runs through 557 km up to Brazilian border
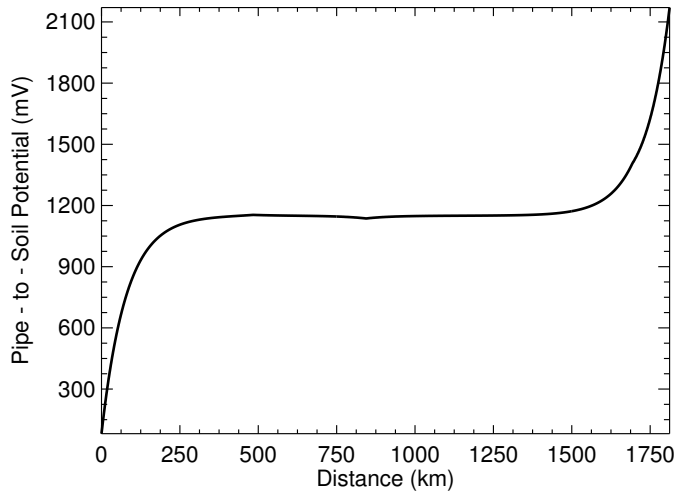
Figure 4. Pipe-to-soil potential obtained by DSLT theory for different sites (values in km at the top) on the GASBOL pipeline for a terminating impedance of 1000 ohms on 17th March 2015 Geomagnetic Storm. Solid lines delimit the safe range of the GASBOL operation.
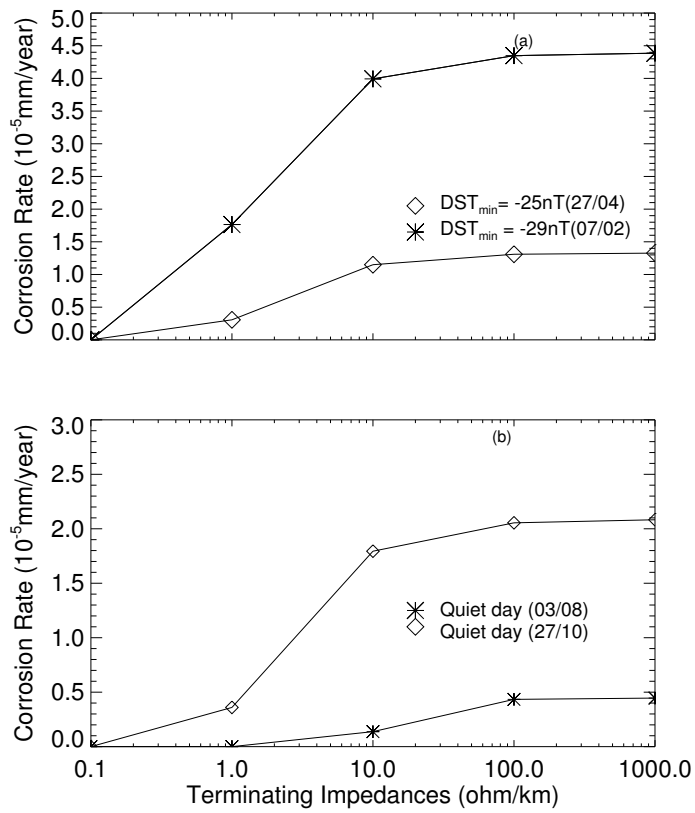
It is possible to observe that in both cases the largest variations in PSP is relative to the largest variations in electric field, that occurred in the main stage of the 17th March geomagnetic storm. The PSP was out of the safe region to low terminating impedance, and mainly when the pipe was considered with high terminating impedance. The terminating impedances are responsible to allow the entrance of GICs in the pipe, and high terminating impedance is relative to the pipe connected to the ground.

From Figures 3 and 4, it was also observed that the largest PSP fluctuations were at the ends of the pipe. This result is confirmed in Figure 5, which is a profile of the PSP as a function of the length of the pipe at 13 UT, on 17th March 2015. This result confirms the mathematical theory described by Boteler and Seager (1998).According to those authors, it produces a movement of electrical charge away from one end and a buildup of charge at the other end, resulting in the S-shaped potential profile observed. At the beginning of the pipe up to 250 km, the negative variation of the potential of the pipe with respect to the ground causes a current to flow onto the pipe. Meanwhile, on the other side, at about 1600 km, positive variation potential causes the current to leave the pipe.
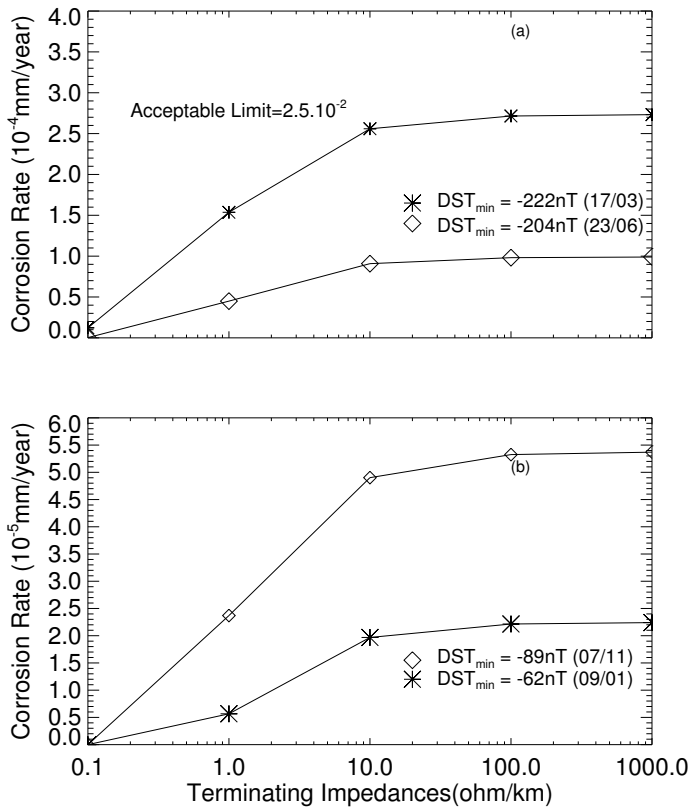
Figure 5. Pipe-to-soil potential profile as function of the distance along the pipeline at 13 UT on 17 March 2015.

Figure 6 and 7 show the corrosion rates in GASBOL as a function of the terminating impedances as well to 8 space weather events in 2015. The corrosion rate was estimated using Equation (3). The events were set by the intense geomagnetic activity, using the DST index. Figures 6 is related to loss of material during strong ($DST_{min} < 100$) and moderated($< -30 < DST_{min} < -100$) geomagnetic storms. Figures 7 shows the weak storms ($DST_{min} < 30$) and quiet days. The markers in Figures 6 and 7 are related to the different event for each level of storm intensity. The acceptable limit to the corrosion rate quoted by Gummow (2002) is $0.025mm/year$.

Figure 6. Corrosion rate as a function of the terminating impedances for strong (a) and moderated(b) geomagnetic storms. The acceptable limit of corrosion is indicated at the top painel.

Figure 7. Corrosion rate as a function of the terminating impedances for weak geomagnetic storms (a) and quite day (b).

In Figure 6a, it is possible to observe that the corrosion rate during strong geomagnetic storms was greater than 0.005 mm/year when the terminating impedances were above the 1 ohms. In addition, the corrosion rate presented constant values to impedances greater than 10 ohms/km. During the 17th March 2015 geomagnetic storm (star), the loss was the greatest for all impedances above the 10 ohms. Figure 6b is relative to moderated storms. It shows that on 7th November 2015 (diamond) the values were greater than 2.10^{-5} mm for impedances equal and greater than 1 ohm/km. These results are close to loss of material observed on 23rd June geomagnetic storm (diamond on the Figure 6a), considered strong, however, the loss of material was not close to the 17th March 2015 storm, which was 10 times greater than the moderated storms.

Figure 7a shows the corrosion rates for weak storms. It is possible to observe that the loss of material on 07th February 2015 geomagnetic storm was close to the result found on 1st January 2015 storm and for impedances greater than 1 ohm, the loss of material was greater. In quiet days (Figure 7b), with no geomagnetic storms, the results were reduced relative to weak storms,

reaching maximum values about 2.10^5 mm in maximum impedances. In general, strong storms have more significant values when compared to weak, moderate and quiet days.

A. Martin (1993) observed corrosion rates in the north region of Australia (similar latitude to Brazil). They found corrosions rate ranging between 0.01 mm/year and 0.038 mm/year. According to the A. Martin (1993), high corrosion rate is responsible for penetration in pipe of 10 % in 14 years. Henriksen et al. (1978) studied a Norway pipeline with 300 telluric events found a corrosion rate of 0.04 mm/year caused by these events.

Considering that geomagnetic storms occur several times a year, primary during the high solar activity periods there would be many days when currents are flowing along the pipes. According to Osella and Favetto (2000) two risks are related to this. One of them is related to the enforcement of the induced current when the pipe is installed in a less conductive medium. This implies that a sector of the pipe would be the anode, and the soil, would be the cathode. This configuration is responsible for the penetration of the excess of currents through the pipe, to the soil. The other risk is associated with the deterioration of the coating caused by high levels of current intensity.

4 Summary

The presented application of the DSLT theory to evaluate the corrosion rate in first Bolivia - Brazil gas pipeline route has provided ways to a new understanding of telluric current effects on the pipeline during extreme space weather events. The use of magnetometer data to compute the electrical field, allows to estimating the PSP and corrosion rate which brought the following conclusions:

1. The electrical field peaks were computed on 17th March geomagnetic storm occurred at the same time of the main stage of the storm, and the currents generated could arrive in Brazil by compressional waves or surface waves.

2. The GASBOL pipeline presented fluctuations in PSP which exceed the cathodic protection levels caused by GICs, mainly in the ends of the pipe with high and low terminating impedances during the 17th March geomagnetic storm.

3. The GASBOL presented significant corrosion levels for terminating impedances greater than 10 ohm/km, mainly in the 17th Geomagnetic Storm. Besides, the event did not exceed the accepetable level, but they can contribute to accelerate the corrosion process of the pipe. Therefore, the effects of GICs in pipelines can not be negligible, even in middle latitudes, since they can reduce the lifetime of a pipeline.

References

A. Fernberg, P., Samson, C., Boteler, D., Trichtchenko, L., and Larocca, P.: Earth conductivity structures and their effects on geomagnetic induction in pipelines, Annales Geophysicae, 25, https://doi.org/10.5194/angeo-25-207-2007, 2007.

A. Martin, B.: Telluric Effects on a Buried Pipeline, Corrosion, 49, 343–350, https://doi.org/10.5006/1.3316059, 1993.

Anderson, C. W., Lanzerotti, L. J., and MacLennan, C. G.: Outage of the l4 system and the geomagnetic disturbances of 4 august 1972, The Bell System Technical Journal, 53, 1817–1837, https://doi.org/10.1002/j.1538-7305.1974.tb02817.x, 1974.

Boteler, D. and Cookson, M.: TELLURIC CURRENTS AND THEIR EFFECTS ON PIPELINES IN THE COOK STRAIT REGION OF NEW ZEALAND., Materials Performance, 25, 27–32, 1986.

Boteler, D. H. and Seager, W. H.: Telluric Currents: A Meeting of Theory and Observation, CORROSION, 54, 751–755, https://doi.org/10.5006/1.3284894, https://doi.org/10.5006/1.3284894, 1998.

Campbell, W. H.: Observation of electric currents in the Alaska oil pipeline resulting from auroral electrojet current sources, Geophysical Journal International, 61, 437–449, 1980.

Denardini, C. M., Chen, S. S., Resende, L. C. A., Moro, J., Bilibio, A. V., Fagundes, P. R., Gende, M. A., Cabrera, M. A., Bolzan, M. J. A., Padilha, A. L., Schuch, N. J., Hormaechea, J. L., Alves, L. R., Barbosa Neto, P. F., Nogueira, P. A. B., Picanço, G. A. S., and Bertollotto, T. O.: The Embrace Magnetometer Network for South America: Network Description and Its Qualification, Radio Science, 53, 288–302, https://doi.org/10.1002/2017RS006477, 2018.

Guillon, S., Toner, P., Gibson, L., and Boteler, D.: A Colorful Blackout: The Havoc Caused by Auroral Electrojet Generated Magnetic Field Variations in 1989, IEEE Power and Energy Magazine, 14, 59–71, https://doi.org/10.1109/MPE.2016.2591760, 2016.

Gummow, R.: GIC effects on pipeline corrosion and corrosion control systems, Journal of Atmospheric and Solar-Terrestrial Physics, 64, 1755–1764, https://doi.org/10.1016/S1364-6826(02)00125-6, 2002.

Heirtzler, J.: The future of the South Atlantic anomaly and implications for radiation damage in space, Journal of Atmospheric and Solar-Terrestrial Physics, 64, 1701–1708, https://doi.org/10.1016/S1364-6826(02)00120-7, 2002.

Henriksen, J., Elvik, R., and Granasen, L.: Telluric current corrosion on buried pipelines, Proceedings of the Eighth Scandinavian Corrosion Congress, Hensinki, 2, 167–176, 1978.

Ingham, M. and J. Rodger, C.: Telluric Field Variations as Drivers of Variations in Cathodic Protection Potential on a Natural Gas Pipeline in New Zealand, Space Weather, 16, https://doi.org/10.1029/2018SW001985, 2018.

Lanzerotti, L. J., D. J., T., and Macleannan, C. G.: Engineering issues in space weather, International Union of Radio Science (URSI), 14, 25–50, 1999.

Marshall, R. A., Waters, C. L., and Sciffer, M. D.: Spectral analysis of pipe-to-soil potentials with variations of the Earth's magnetic field in the Australian region, Space Weather, 8, https://doi.org/10.1029/2009SW000553, https://agupubs.onlinelibrary.wiley.com/doi/abs/10.1029/2009SW000553, 2010.

Osella, A. and Favetto, A.: Effects of soil resistivity on currents induced on pipelines, Journal of Applied Geophysics, 44, 303 – 312, https://doi.org/https://doi.org/10.1016/S0926-9851(00)00008-2, http://www.sciencedirect.com/science/article/pii/S0926985100000082, 2000.

Osella, A., Favetto, A., and Lopez, E.: Currents induced by geomagnetic storms on buried pipelines as a cause of corrosion, Journal of Applied Geophysics - J APPL GEOPHYS, 38, 219–233, https://doi.org/10.1016/S0926-9851(97)00019-0, 1998.

Padilha, A., Trivedi, N., Vitorello, I., and da Costa, J.: Geophysical constraints on tectonic models of the Taubaté Basin, southeastern Brazil, Tectonophysics, 196, 157 – 172, https://doi.org/https://doi.org/10.1016/0040-1951(91)90294-3, http://www.sciencedirect.com/science/article/pii/0040195191902943, 1991.

Paulikas, G. A.: Precipitation of particles at low and middle latitudes, Reviews of Geophysics, 13, 709–734, https://doi.org/10.1029/RG013i005p00709, https://agupubs.onlinelibrary.wiley.com/doi/abs/10.1029/RG013i005p00709, 1975.

Place, T. and Sneath, T.: Practical telluric compensation for pipeline close-interval surveys, 40, 22–27, 2001.

Pulkkinen, A., Pirjola, R., Boteler, D., Viljanen, A., and Yegorov, I.: Modelling of space weather effects on pipelines, Journal of Applied Geophysics, 48, 233 – 256, https://doi.org/https://doi.org/10.1016/S0926-9851(01)00109-4, http://www.sciencedirect.com/science/article/pii/S0926985101001094, 2001.

Schelkunoff, S. A.: Electromagnetic waves / by S.A. Schelkunoff, Van Nostrand New York, 1943.

Seager, W.: Adverse telluric effects on northern pipelines, International Arctic Technology Conference, Anchorage, Alaska, 2, 1991.

Trichtchenko, L. and Boteler, D.: Modelling of geomagnetic induction pipelines, Annales Geophysicae, 20, https://doi.org/10.5194/angeo-20-1063-2002, 2002.

Trivedi, N., Pathan, B., Schuch, N. J., Barreto, M., and Dutra, L.: Geomagnetic phenomena in the South Atlantic anomaly region in Brazil, Advances in Space Research, 36, 2021 – 2024, https://doi.org/https://doi.org/10.1016/j.asr.2004.09.020, http://www.sciencedirect.com/science/article/pii/S0273117705004862, solar Wind-Magnetosphere-Ionosphere Dynamics and Radiation Models, 2005.